

SEGSPAT: FEED-FORWARD GAUSSIAN SPLATTING AND OPEN-SET SEMANTIC SEGMENTATION

Peter Siegel
ETH Zürich
psiegel@ethz.ch

Federico Tombari
Google
dbarath@inf.ethz.ch

Marc Pollefeys
ETH Zürich, Microsoft
dbarath@inf.ethz.ch

Daniel Barath
ETH Zürich
dbarath@inf.ethz.ch

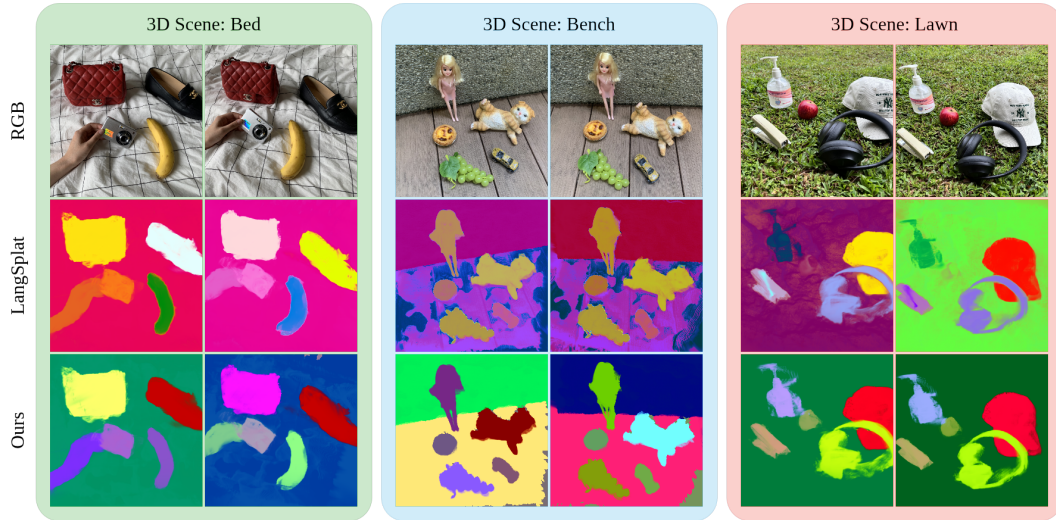


Figure 1: Visualization of learned 3D language features of the previous state-of-the-art method, LangSplat Qin et al. (2024), and our SegSplat. While LangSplat requires per-scene training and generates imprecise features, our SegSplat captures smooth regions more consistently and needs *no* training. While being effective, our SegSplat is also 59× faster than LangSplat.

ABSTRACT

Efficient 3D scene reconstruction with open-set semantic understanding is vital for robotics and augmented reality. However, existing methods either require costly per-scene optimization to incorporate semantics into expressive 3D representations like 3D Gaussian Splat (3DGS), or, if feed-forward, focus predominantly on geometry and appearance. This paper introduces SegSplat, the first framework to predict 3D Gaussian Splat with associated open-set semantic features in a purely feed-forward manner. Building upon efficient sparse-view 3DGS techniques, SegSplat uniquely integrates semantic knowledge derived from 2D open-set segmentation models (e.g., SAM and CLIP) without any training. We achieve this by constructing a compact semantic memory bank from features in the input images and assigning each Gaussian a discrete index to this bank. This approach enables rich semantic feature association with minimal additional storage and computational overhead, thus preserving the rapid inference capabilities of feed-forward 3DGS. We demonstrate that SegSplat delivers geometric fidelity comparable to state-of-the-art feed-forward reconstruction methods while simultaneously enabling versatile open-set semantic querying, all without necessitating scene-specific optimization. Our work bridges a critical gap, paving the way for practical, on-the-fly generation of semantically rich 3D environments.

1 INTRODUCTION

The ability to reconstruct 3D environments with rich, open-set semantic understanding is increasingly critical for intelligent systems, enabling applications ranging from robotic navigation to immersive augmented reality. These scenarios demand not only accurate geometry but also the capacity to identify, query, and manipulate arbitrary high-level concepts – such as “a specific type of chair”, “any vehicle”, or “all metallic objects” – directly within the 3D representation Kerr et al. (2023). While progress has been made in both 3D reconstruction Mildenhall et al. (2020); Yu et al. (2021); Kerbl et al. (2023) and 2D open-set semantic segmentation Xu et al. (2023); Li et al. (2022); Liang et al. (2023), integrating these capabilities into a unified and efficient 3D representation that supports open-vocabulary queries without per-scene fine-tuning remains a fundamental challenge.

Recent advances in neural rendering, particularly Neural Radiance Fields (NeRFs) Mildenhall et al. (2020), have demonstrated compelling view synthesis through implicit scene representations. However, their reliance on per-scene optimization limits scalability and real-time deployment. In contrast, 3D Gaussian Splatting (3DGS) Kerbl et al. (2023) represents scenes as collections of 3D Gaussians, enabling high-quality, real-time rendering. Despite these rendering advantages, training times remain substantial Kerbl et al. (2023), motivating a shift towards faster feed-forward approaches Xu et al. (2024); Chen et al. (2024); Ye et al. (2024a).

To bridge the semantic gap, recent works extend 3DGS with language-aligned features Qin et al. (2024); Shi et al. (2023); Ye et al. (2024b), typically associating each Gaussian with a feature vector (e.g., from CLIP Radford et al. (2021)). These enable open-vocabulary querying, but most methods still depend on per-scene optimization (first constructing the 3DGS, then fitting semantic features), making them ill-suited for dynamic or large-scale environments.

This paper introduces SegSplat, a novel framework that predicts 3D Gaussian Splats enriched with open-set semantic features in a single feed-forward pass. Building on recent progress in sparse-view 3DGS reconstruction, we leverage the DepthSplat architecture Xu et al. (2024) for fast and robust geometric prediction. Our key contribution is the seamless integration of semantic information, extracted via 2D open-set segmentation models (e.g., SAM Kirillov et al. (2023) with CLIP), directly into the predicted Gaussians.

To achieve this, we construct a compact semantic memory bank from features observed in the input views and assign a discrete index (analogous to a one-hot code) to each 3D Gaussian primitive. This allows each Gaussian to reference a powerful semantic descriptor while introducing minimal storage and computational overhead, preserving fast inference.

In summary, SegSplat provides a unified, efficient pipeline that jointly reconstructs 3D scene geometry and embeds open-vocabulary semantic features – eliminating the need for per-scene optimization. We validate our method on challenging datasets including 3D-OVS Liu et al. (2023a) and RealEstate10k Zhou et al. (2018), demonstrating that SegSplat achieves accurate feed-forward 3DGS quality while enabling robust open-set semantic querying.

2 RELATED WORK

Our work integrates progress in three key areas: 3D scene representations, their accelerated sparse feed-forward generation, and the incorporation of open-vocabulary semantic understanding. This review situates SegSplat’s contribution: a method for feed-forward generation of 3D Gaussian Splatting (3DGS) models with associated open-set semantic features.

The pursuit of high-fidelity 3D scene models have evolved from traditional representations like meshes, which often involve complex creation pipelines, towards learnable techniques. Neural Radiance Fields (NeRF) Mildenhall et al. (2020) were a significant advance, using neural networks to synthesize photorealistic novel views. However, NeRFs typically require lengthy per-scene optimization, limiting their practical use. 3D Gaussian Splatting (3DGS) Kerbl et al. (2023) offered a compelling alternative, explicitly representing scenes with 3D Gaussian primitives. This approach achieves state-of-the-art visual quality and real-time rendering via a differentiable rasterizer, making 3DGS a strong foundation for complex scene understanding tasks. However, such approaches still require expensive per-scene optimizations.

To address the computational demands of this per-scene optimization, research has shifted towards feed-forward methods that generate 3D representations in a single feed-forward pass from a sparse input images. These models are trained on large datasets to predict scene parameters directly. For 3DGS, methods like MVSplat Chen et al. (2024), DepthSplat Xu et al. (2024), and NoPoSplat Ye et al. (2024a) demonstrate rapid reconstruction by employing pipelines that typically involve 2D feature extraction, geometric inference (e.g., depth estimation), and regression of Gaussian attributes. While these approaches efficiently reconstruct geometry and appearance, they do not inherently produce semantic information. Integrating semantics requires separate, post-hoc processing.

Incorporating semantic understanding into 3D models is crucial for higher-level reasoning. A common strategy is to "lift" features or predictions from powerful pre-trained 2D foundation models, such as CLIP Radford et al. (2021) for image-text understanding and SAM Kirillov et al. (2023) for class-agnostic segmentation. Projecting or distilling information from these 2D models into 3D representations is effective but presents challenges, including maintaining multi-view consistency and handling occlusions.

Several works have focused on creating 3D representations that store and query semantic information. For NeRFs, LERF Kerr et al. (2023) enabled open-vocabulary querying by distilling CLIP features into a 3D language field, but this process requires per-scene optimization for the semantic component. Similar efforts for 3DGS, such as LangSplat Qin et al. (2024) and LEGaussians Shi et al. (2023), associate language features with Gaussian primitives, also relying on per-scene optimization to embed these semantics.

The high dimensionality of language features stored within each Gaussian makes it computationally expensive for language-embedded 3DGS methods to rasterize them directly Qin et al. (2024). To address this issue various compression and quantization strategies have been proposed. LangSplat adopts a pretrained scene-specific autoencoder Qin et al. (2024) to compress the language features into a lower-dimensional space used for rasterization. After novel view rendering, the autoencoder is used to decode the language features to their original size. LEGaussians uses quantized language feature index maps to avoid storing and rasterizing a full language feature for each Gaussian Shi et al. (2023). A low-dimensional semantic feature vector is added to each gaussian which is then decoded into a discrete index in the feature index map using a small scene-specific MLP after the rasterization step.

Gaussian Grouping Ye et al. (2024b) reparametrizes the open-set segmentation problem as a generic object segmentation task. It learns an identity encoding for each Gaussian representing object associations from video-tracked object masks found in the input images. Because each gaussian is not directly imbued with any open-set semantic features this approach requires a secondary step where a 2D object detection model such as GroundingDINO Liu et al. (2023b) is used to associate a text prompt with a 3D object in the scene. While methods like LBG Chacko et al. (2025) offer training-free mechanisms to add semantics to pre-existing 3DGS models, they depend on an already reconstructed geometric model and do not integrate semantic generation with geometric reconstruction.

Many existing methods for semantic 3D scene understanding, thus, face a bottleneck: even if geometry is reconstructed quickly, embedding rich semantic features often requires a separate, computationally intensive per-scene optimization step. This limits their applicability in scenarios demanding rapid, on-the-fly generation of semantic 3D models. SegSplat directly addresses this limitation. It proposes a framework to predict both 3D Gaussian Splat geometry and associated open-set semantic features in a single feed-forward pass from sparse image inputs tailored to the 3DGS representation produced by feed-forward gaussian splatting. This concurrent generation of geometry and semantics, without per-scene semantic optimization, is the key distinction of our approach.

3 PROPOSED METHOD

Our proposed method, SegSplat, enables feed-forward generation of 3D Gaussian Splatting (3DGS) representations augmented with open-set semantic features from sparse multi-view images. The core idea is to: (1) construct a semantic feature bank by leveraging Segment Anything Model (SAM) and CLIP extracted from input views, followed by clustering to identify representative semantic concepts. (2) Utilize a feed-forward model (DepthSplat) to generate 3D Gaussian primitives, where

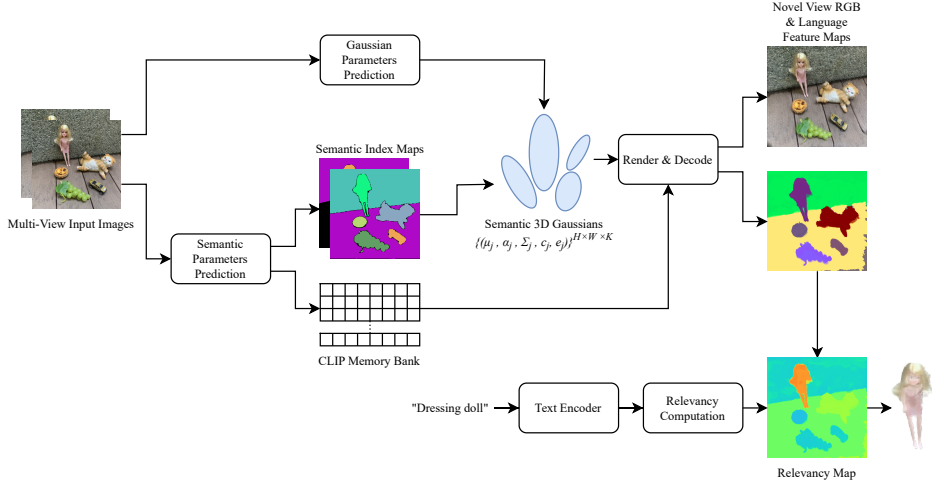


Figure 2: **SegSplat** predicts 3D Gaussian splats embedded with language features from sparse multi-view images, without any training. Our pipeline leverages pretrained DepthSplat to estimate 3D Gaussian parameters per pixel, and uses SAM+CLIP to extract segmentation masks and CLIP embeddings. To ensure memory efficiency, we construct a CLIP feature memory bank and represent per-object semantics using one-hot index maps aligned with this bank. These semantic indices are appended to the Gaussians predicted by DepthSplat. After splatting, we reconstruct full-length language features via an element-wise product between the rendered index maps and the memory bank. Novel-view querying is then performed on the decoded CLIP feature image.

each primitive is associated with a semantic index corresponding to an entry in our feature bank. (3) Render both appearance and semantic features for novel views, enabling open-vocabulary querying.

3.1 SEMANTIC PARAMETER PREDICTION

The aim of this component of the pipeline is to represent semantic information found in the input images with a memory bank of CLIP features and corresponding per-pixel semantic indices. This memory bank will allow to have an efficient Gaussian-to-semantic assignment by simply assigning the index of the semantics from the bank to a given Gaussian primitive. Given K input images $\{\mathbf{I}_k \in \mathbb{R}^{H \times W \times 3}\}_{k=1}^K$ and their corresponding camera projection matrices $\{\mathbf{P}_k \in \mathbb{R}^{3 \times 4}\}_{k=1}^K$, we perform the following steps:

1. **Mask Extraction:** For each input image \mathbf{I}_k , we employ SAM Kirillov et al. (2023) to generate a set of N_k object masks $\{\mathbf{m}_{ki} \subset \mathbb{R}^2\}_{i=1}^{N_k}$. We prompt SAM at a “whole” object granularity and apply non-maximum suppression to ensure minimal overlap between masks. Each pixel (u, v) in image \mathbf{I}_k is thus associated with at most one mask.
2. **CLIP Feature Extraction:** For each mask \mathbf{m}_{ki} , we create a cropped image patch. Pixels outside the mask \mathbf{m}_{ki} within this crop are zeroed out. We then compute a D_{CLIP} -dimensional CLIP image embedding $\mathbf{f}_{ki} \in \mathbb{R}^{D_{\text{CLIP}}}$ using a pre-trained CLIP image encoder Radford et al. (2021). This yields a collection of $N_{\text{total}} = \sum_{k=1}^K N_k$ mask-specific CLIP features.
3. **Clustering and Bank Formation:** To create a concise semantic representation, we pool all N_{total} CLIP features $\{\mathbf{f}_{ki}\}$. We then apply K-Means clustering to group these features into M semantic clusters. The centroids of these M clusters form our semantic feature bank $\mathbf{B} = [\mathbf{b}_1, \dots, \mathbf{b}_M]^T \in \mathbb{R}^{M \times D_{\text{CLIP}}}$ used in later processes. Each original CLIP feature \mathbf{f}_{ki} is assigned to its closest cluster centroid \mathbf{b}_m .
4. **Per-Pixel Semantic Index Maps:** Using the bank, we generate a semantic index map $\mathbf{S}_k \in \{1, \dots, M\}^{H \times W}$ for each input image \mathbf{I}_k . For a pixel (u, v) in \mathbf{I}_k belonging to mask \mathbf{m}_{ki} (assigned to cluster m), we set $\mathbf{S}_k(u, v) = m$. Pixels not belonging to any mask are assigned a background index 0. This results in K semantic index maps $\{\mathbf{S}_k\}_{k=1}^K$.

3.2 FEED-FORWARD GENERATION OF SEMANTIC GAUSSIANS

We adopt a feed-forward Gaussian Splatting architecture, specifically a frozen DepthSplat model Xu et al. (2024), to generate the 3D scene representation. Beginning with K sparse input images $\{\mathbf{I}_i\}_{i=1}^K$, ($\mathbf{I}^i \in \mathbb{R}^{H \times W \times 3}$), and their corresponding camera projection matrices $\{\mathbf{P}_i\}_{i=1}^K$, ($\mathbf{P}^i \in \mathbb{R}^{3 \times 4}$), DepthSplat predicts the per-pixel Gaussian parameters $\{(\boldsymbol{\mu}_j, \alpha_j, \boldsymbol{\Sigma}_j, \mathbf{c}_j)\}_{j=1}^{H \times W \times K}$ for each image. Gaussian parameters $\boldsymbol{\mu}_j$, α_j , $\boldsymbol{\Sigma}_j$, and \mathbf{c}_j denote the 3D Gaussians position, opacity, covariance, and color (represented as spherical harmonics), respectively.

Because DepthSplat predicts per-pixel Gaussian parameters for each pixel in each input view, we can directly append a computed one-hot semantic encoding \mathbf{e}_j derived from the semantic index maps calculated in Section 3.1 to the other Gaussian parameters. Our full Gaussian splatting representation becomes $\mathbf{g}_j = \{(\boldsymbol{\mu}_j, \alpha_j, \boldsymbol{\Sigma}_j, \mathbf{c}_j, \mathbf{e}_j)\} \in \mathbb{R}_{j=1}^{H \times W \times K}$. Such a representation allows for the light-weight assignment of semantics to Gaussians without significantly inflating the number of parameters that need to be stored for each primitive. By the end of this step, each Gaussian has a corresponding semantic class assigned.

3.3 DIFFERENTIABLE RENDERING OF COLOR AND SEMANTICS

To synthesize a novel view given a camera pose $\mathbf{P}_{\text{novel}}$, we use the standard tile-based 3D Gaussian splatting rasterization process Kerbl et al. (2023). For each pixel v in the novel view it is the following.

Color Rendering: For each pixel v , the color $C(v) \in \mathbb{R}^3$ is rendered as follows:

$$C(v) = \sum_{i \in \mathcal{N}} c_i \alpha_i \prod_{j=1}^{i-1} (1 - \alpha_j), \quad (1)$$

where c_i denotes the color of the i -th Gaussian, \mathcal{N} is the set of Gaussians within a tile, and $\alpha_i = o_i G_i^{2D}(v)$, with o_i being the opacity of the i -th Gaussian and $G_i^{2D}(\cdot)$ denoting the projection of the i -th Gaussian onto 2D.

Semantic Index Rendering: Each 3D Gaussian G_j in our scene representation is associated with a one-hot semantic vector $\mathbf{e}_j \in \{0, 1\}^M$, indicating its assignment to one of the M semantic concepts derived from our feature bank. To render the semantic information at a pixel in a novel view, we adapt the splatting mechanism used for color as follows:

$$\mathbf{E}(v) = \sum_{i \in \mathcal{N}} \mathbf{e}_i \alpha_i \prod_{j=1}^{i-1} (1 - \alpha_j), \quad (2)$$

where $\mathbf{E}(v)$ represents the semantic embedding rendered at pixel v . This vector $\mathbf{E}(v)$ represents a blended distribution of semantic concepts at the pixel, where each element $(\mathbf{E}(v))_m$ indicates the aggregated presence of the m -th semantic concept.

CLIP Feature Map Recovery: After rendering, each pixel possesses a blended semantic vector $\mathbf{E}(v) \in \mathbb{R}^M$. Our semantic feature bank $\mathbf{B} \in \mathbb{R}^{M \times D_{\text{CLIP}}}$ stores the D_{CLIP} -dimensional CLIP embeddings for the M representative semantic concepts (i.e., the m -th row of \mathbf{B} , denoted \mathbf{b}_m^T , is the CLIP feature vector for the m -th semantic concept). To recover a continuous CLIP feature vector $\mathbf{F}(v) \in \mathbb{R}^{D_{\text{CLIP}}}$ for the pixel, we use $\mathbf{E}(v)$ to linearly combine the feature vectors stored in the bank \mathbf{B} . Specifically, the m -th component of $\mathbf{E}(v)$, $(\mathbf{E}(v))_m$, acts as the weight for the m -th semantic feature vector \mathbf{b}_m as follows:

$$\mathbf{F}(v) = \sum_{m=1}^M (\mathbf{E}(v))_m \cdot \mathbf{b}_m = \mathbf{E}(v)^T \mathbf{B}. \quad (3)$$

This operation effectively translates the rendered (potentially mixed) semantic indices back into the rich, continuous CLIP feature space. The resulting $\mathbf{F}(v)$ for all pixels forms a dense CLIP feature map for the novel view, which can then be used for open-vocabulary tasks.

As a result, the contributions of each CLIP feature in the memory bank is weighted by the rendered mask encoding. Finally, before performing open-vocabulary querying, the CLIP features are normalized to unit length.

3.4 OPEN-VOCABULARY QUERYING

With the rendered CLIP feature map $\mathbf{F}(v)$, we can perform open-vocabulary queries. Given a text query q_{text} , we compute its CLIP text embedding $\phi_{qry} \in \mathbb{R}^{D_{\text{CLIP}}}$. For each pixel with rendered CLIP image feature $\phi_{\text{img}} = \mathbf{F}(v)$, we calculate a relevancy score following LERF Kerr et al. (2023) as:

$$\text{relevancy}(\phi_{\text{img}}, \phi_{qry}) = \min_{i \in \{\text{obj, thg, stf}\}} \left(\frac{\exp(\tau \cdot \phi_{\text{img}} \cdot \phi_{qry})}{\exp(\tau \cdot \phi_{\text{img}} \cdot \phi_{qry}) + \exp(\tau \cdot \phi_{\text{img}} \cdot \phi_{i_{\text{canon}}})} \right) \quad (4)$$

where $\phi_{i_{\text{canon}}}$ are CLIP text embeddings of predefined canonical phrases like “object”, “things”, “stuff”, and τ is a temperature parameter. Relevancy scores below a predefined threshold (e.g., 0.5) are set to 0, and the remaining scores can be further thresholded to obtain fine-grained segmentation masks corresponding to the input query.

4 EXPERIMENTS

In this section, we evaluate our method on standard benchmarks for 3D open-set semantic segmentation, and we also demonstrate that SegSplat achieves the same photometric scores as the state-of-the-art DepthSplat.

Datasets. We evaluate our method on two datasets: RealEstate10K (RE10k) (Zhou et al., 2018) and 3D-OVS (Liu et al., 2023a). RE10k comprises a large collection of real estate videos with estimated camera parameters. For RE10k, we use an official subset and follow the train/test split of DepthSplat (Xu et al., 2024). As RE10k lacks mask-level annotations, we present qualitative results for semantic segmentation.

3D-OVS (Liu et al., 2023a) features scenes with long-tailed object distributions in diverse backgrounds. For sparse multi-view reconstruction on 3D-OVS, we adopt the train/test split generation methodology from MVsplat (Chen et al., 2024) and DepthSplat (Xu et al., 2024). Our test split uses input views with at least 60% projected overlap; target views are those containing ground-truth semantic labels. We report Intersection over Union (IoU) for 3D semantic segmentation on 3D-OVS.

Baselines. We compare SegSplat against several state-of-the-art methods. It is crucial to distinguish between methods that perform per-scene optimization or require access to the *entire scene context* for semantic understanding, and feed-forward approaches like ours that operate on a *limited set of input views* (typically two in our experiments).

First, we consider baselines that leverage extensive information from the target scene, often through per-scene training or optimization. Consequently, they are expected to achieve higher accuracy and primarily serve as a reference for the semantic segmentation task, rather than direct competitors to our feed-forward approach. This group includes open-vocabulary 2D segmentation models such as LSeg (Li et al., 2022), ODISE (Xu et al., 2023), and OV-Seg (Liang et al., 2023), for which metrics are typically derived from individual views without enforcing 3D multi-view consistency. We also include NeRF-based methods like FFD (Kobayashi et al., 2022), LERF (Kerr et al., 2023), and 3D-OVS (Liu et al., 2023a), requiring per-scene optimization. Furthermore, non-feed-forward Gaussian Splatting semantic methods such as GS-Grouping (Ye et al., 2024b), and LangSplat (Qin et al., 2024) fall into this category, as they typically operate on or optimize semantic features for a 3DGS scene representation, benefiting from full scene context.

Second, to ensure a fair comparison for our feed-forward SegSplat, we create a feed-forward comparison group. For this, we adapt the state-of-the-art LangSplat (Qin et al., 2024) to operate within the same feed-forward, sparse-view framework as SegSplat. Instead of using the pre-trained or optimized 3DGS representations from their original implementations, LangSplat is initialized using the exact same Gaussians predicted by our common frozen DepthSplat backbone from only two input views. All methods in this group utilize identical semantic features extracted from SAM (masks) and CLIP (embeddings) as input. LangSplat requires a scene-specific autoencoder. We train it for each scene individually (2k iterations, batch size 2, learning rate 2.0×10^{-2} , AdamW optimizer). The time taken for this per-scene autoencoder training is factored into LangSplat’s reported run-time to ensure a fair comparison against methods that do not require scene-specific training.

Implementation details. Our pipeline utilizes the 37M parameter DepthSplat model, pre-trained on RE10k with 256×256 resolution images, to predict initial Gaussian parameters. The DepthSplat

Table 1: **3D semantic segmentation** performance comparison (mIoU %) on the 3D-OVS dataset (Liu et al., 2023a). Methods are grouped by their operational principle. Best results within the feed-forward category (run only on two input views) and leading results among contextual (non-feed-forward; trained on *all* images from a scene) methods are shown in **bold**.

Principle	Method	Bed	Bench	Room	Sofa	Lawn	Overall
2D Image Segmentation	LSeg (Li et al., 2022)	56.0	6.0	19.2	4.5	17.5	20.6
	ODISE (Xu et al., 2023)	52.6	24.1	52.5	48.3	39.8	43.5
	OV-Seg (Liang et al., 2023)	79.8	88.9	71.4	66.1	81.2	77.5
NeRF	FFD (Kobayashi et al., 2022)	56.6	6.1	25.1	3.7	42.9	26.9
	LERF (Kerr et al., 2023)	73.5	53.2	46.6	27.0	73.7	54.8
	3D-OVS (Liu et al., 2023a)	89.5	89.3	92.8	74.0	88.2	86.8
Gaussian Splatting	GS-Grouping (Ye et al., 2024b)	83.0	91.5	85.9	87.3	90.6	87.7
	LangSplat (Qin et al., 2024)	92.5	94.2	94.1	90.0	96.1	93.4
Feed-Forward GS	LangSplat (Qin et al., 2024)	59.4	75.1	7.2	50.9	46.0	47.7
	SegSplat	66.2	75.9	19.8	64.5	80.8	61.4

Table 2: **Novel view synthesis quality** for SegSplat and its base geometric model, DepthSplat, on the RE10k and 3D-OVS datasets. Metrics reported are PSNR↑, SSIM↑, and LPIPS↓. The identical performance demonstrates that SegSplat’s method of integrating semantic features does not degrade the geometric and appearance reconstruction fidelity of the underlying DepthSplat model, as SegSplat utilizes the same Gaussian parameters for rendering.

Dataset	Method	PSNR ↑	SSIM ↑	LPIPS ↓
3D-OVS (Liu et al., 2023a)	DepthSplat (Xu et al., 2024)	16.99	0.392	0.428
	SegSplat	16.99	0.392	0.428
RE10K (Zhou et al., 2018)	DepthSplat (Xu et al., 2024)	25.89	0.881	0.122
	SegSplat	25.89	0.881	0.122

model is not fine-tuned on 3D-OVS, allowing us to evaluate the zero-shot generalization of our semantic assignment approach. To ensure view-invariant semantic rendering, the spherical harmonics degree for the semantic index encoding is set to zero during rasterization. We replace DepthSplat’s original rasterizer (Kerbl et al., 2023) with `gspplat` (Ye et al., 2025) for rendering both color and our semantic index encodings.

For mask extraction from input images (Section 3.1), we employ the SAM ViT-H model (Kirillov et al., 2023). We use the CLIP ViT-B/16 model (Radford et al., 2021), trained on the LAION-2B English subset of LAION-5B (Schuhmann et al., 2022), to extract features from SAM-identified objects and to encode text prompts. The number of clusters M for K-Means during semantic feature bank construction (Section 3.1) is $M = \lambda N_{\text{total}}/K$ where N_{total} is the total number of masks from all K input views, and $\lambda = 1.2$. This heuristic aims to accommodate varying object visibility across views. For open-vocabulary querying (Section 3.4), relevancy scores are computed as in LERF (Kerr et al., 2023). Scores below 0.5 are set to 0. The resulting relevancy map is then thresholded at 0.5 to produce binary segmentation masks.

All experiments are conducted on an NVIDIA RTX-5090 GPU, and we report inference/processing times. The primary evaluation of SegSplat’s performance and efficiency should be made against other methods within the “Feed-Forward GS”, as they operate under similar constraints.

4.1 RESULTS

3D Semantic Segmentation Performance. We evaluated open-vocabulary 3D semantic segmentation capabilities of the proposed SegSplat on the 3D-OVS dataset, with results presented in Table 1. The methods are benchmarked using mean Intersection over Union (mIoU) and are categorized based on their underlying methodology. Examples are shown in Figs. 3, 4 and 5.

The table includes several baselines that perform per-scene optimization or leverage extensive information from the target scene. These encompass 2D image segmentation techniques (LSeg, ODISE, OV-Seg), NeRF-based semantic methods (FFD, LERF, 3D-OVS), and Gaussian Splatting approaches

that optimize semantics for the entire scene (GS-Grouping, LangSplat). These methods, such as the original LangSplat which achieves an overall mIoU of 93.4%, provide a strong performance reference due to their comprehensive access to scene data.

Our primary evaluation focuses on the feed-forward Gaussian Splatting (Feed-Forward GS) category, which operates under the constraint of using only a few input images (two in our setup) without any per-scene optimization for semantics. Within this challenging setting, SegSplat achieves an overall mIoU of 61.4%. This significantly surpasses the adapted feed-forward version of LangSplat, which scores 47.7% mIoU when constrained to the same feed-forward pipeline using an identical DepthSplat backbone and semantic inputs. SegSplat demonstrates superior performance across the majority of reported object categories in this direct comparison, underscoring its efficacy in generating robust semantic segmentations in a single pass.

While a performance difference exists between feed-forward approaches like SegSplat and methods that utilize full scene context and optimization, SegSplat establishes a strong baseline for efficient, open-set semantic understanding with 3D Gaussian Splatting in a purely feed-forward manner. Moreover, it does not require additional per-scene training as LangSplat does.

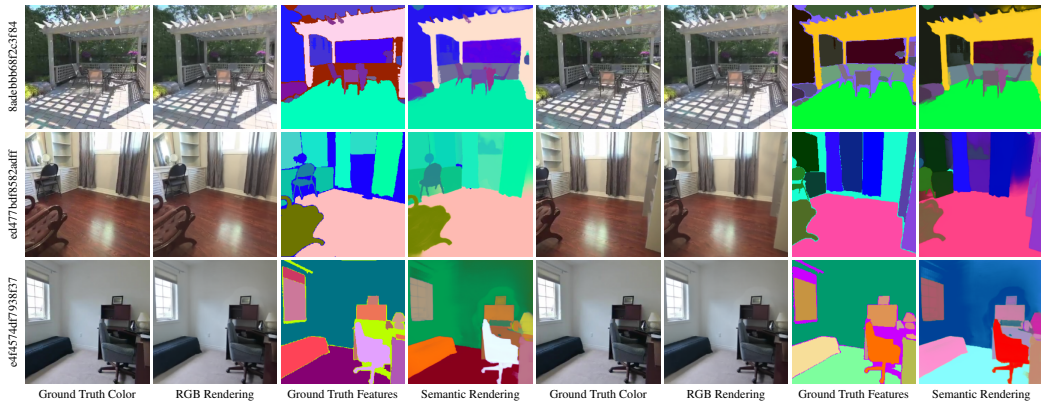


Figure 3: Comparison of predicted and ground truth (GT) color and semantic maps for novel views rendered by SegSplat on the RealEstate10K dataset Zhou et al. (2018). Semantic maps are visualized using PCA. Ground truth semantic features are obtained by applying SAM+CLIP to the corresponding GT novel view images. Each group of four columns shows: GT RGB image, SegSplat-rendered RGB, GT semantics, and SegSplat-rendered semantics. This sequence is repeated for a second novel view.

Table 3 reports open-set 3D semantic segmentation results on the ScanNet++ dataset (Yeshwanth et al., 2023). SegSplat achieves the highest mean IoU among feed-forward approaches. We compare against the recent SAB3R variants (Chen et al., 2025) and LSM (Fan et al., 2024). SegSplat with SAM attains 26.0 percent mIoU and surpasses prior feed-forward baselines by a clear margin. EfficientSAM reduces preprocessing time from 9.70 seconds to 0.98 seconds with a moderate decrease in accuracy, which shows that SegSplat remains effective when using faster mask extraction. Replacing the DepthSplat backbone with MVsplat yields 22.2 percent mIoU, demonstrating that SegSplat generalizes across feed-forward Gaussian Splatting backbones. Inference remains 0.03 seconds for all SegSplat variants.

Geometric Reconstruction Quality. We evaluated whether the integration of our semantic component affects the underlying novel view synthesis quality. SegSplat utilizes the geometric and appearance parameters for its Gaussians directly from the frozen DepthSplat model. The primary goal of this comparison is to demonstrate that our method for adding semantic features preserves the rendering fidelity of the base model.

Table 2 presents standard image quality metrics (PSNR, SSIM and LPIPS) for SegSplat and baseline DepthSplat in the 3D-OVS and RE10k datasets. As shown, SegSplat achieves identical performance to DepthSplat across all metrics on both datasets. This confirms that our approach for incorporating open-set semantic understanding does not introduce any degradation to the high-fidelity geometric and appearance reconstruction capabilities provided by the underlying feed-forward 3DGS model.

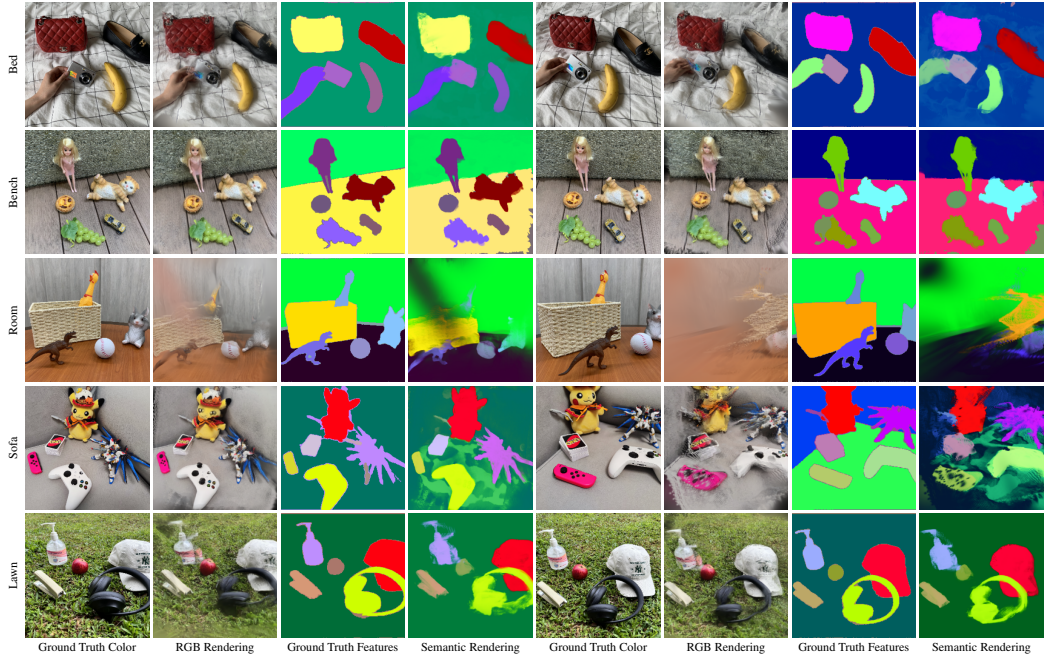


Figure 4: Comparison of predicted and ground truth (GT) color and semantic maps for novel views rendered by SegSplat on the 3D-OVS dataset Liu et al. (2023a). Semantic maps are visualized using PCA. Ground truth semantic features are obtained by applying SAM+CLIP to the corresponding GT novel view images. Each group of four columns shows: GT RGB image, SegSplat-rendered RGB, GT semantics, and SegSplat-rendered semantics. This sequence is repeated for a second novel view.

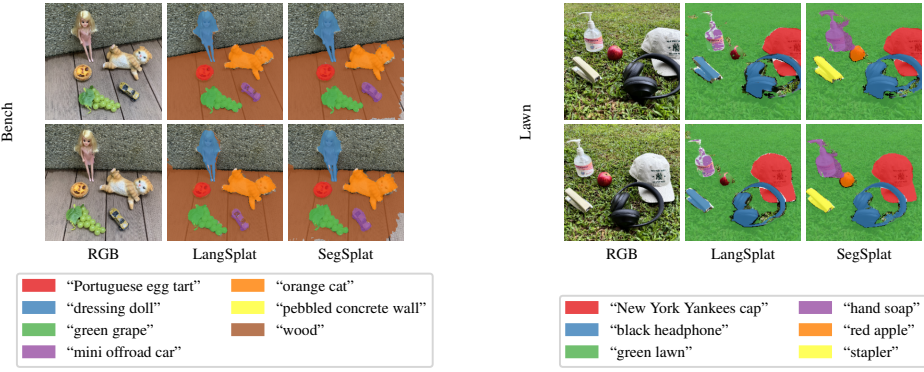


Figure 5: A qualitative comparison of the masks produced by SegSplat and LangSplat on the 3D-OVS dataset Liu et al. (2023a). We show results for two scenes and two different novel views. We observe that our method produces more accurate segmentation masks.

Processing Time. Table 4 presents a detailed runtime comparison of SegSplat and LangSplat, measured on a single RTX 5090 GPU. While both methods require initial 2D semantic feature extraction using SAM+CLIP – which accounts for the majority of the offline cost – SegSplat eliminates the need for scene-specific optimization by performing semantic-to-Gaussian assignment in a single feed-forward pass. In contrast, LangSplat relies on an expensive 565-second scene-specific training stage for semantic association. Excluding shared preprocessing, SegSplat achieves a total inference-time runtime of under 0.2 seconds, over three orders of magnitude faster than LangSplat.

Table 3: Open-set 3D semantic segmentation results on ScanNet++ (Yeshwanth et al., 2023). SegSplat achieves the highest mean IoU among feed-forward methods while retaining low inference time. We report results for SegSplat using EfficientSAM (Xiong et al., 2024) and also using an MVSplat (Chen et al., 2024) backbone. Preprocessing time corresponds to SAM-based mask extraction.

Method	mean IoU (%)	Training	Preprocessing	Inference
SAB3R (B) (Chen et al., 2025)	4.6	not reported	–	≤ 0.108 s
SAB3R (C) (Chen et al., 2025)	17.3	not reported	–	≤ 0.108 s
SAB3R (CD) (Chen et al., 2025)	17.5	not reported	–	≤ 0.108 s
LSM (Fan et al., 2024)	21.4	3 days on $8 \times$ A100	–	0.108 s
SegSplat (SAM)	26.0	–	9.70 s	0.030 s
SegSplat (E-SAM (Xiong et al., 2024))	21.2	–	0.98 s	0.030 s
SegSplat w/ MVSplat	22.2	–	9.70 s	0.030 s

Table 4: **Runtime breakdown of SegSplat and LangSplat (in seconds).** Per-component runtime on the 3D-OVS dataset measured on a single RTX 5090 GPU and averaged after two warm-up batches. LangSplat needs scene-specific training (over 9 mins per scene) before inference, while SegSplat performs all steps in a single feed-forward pass. After SAM+CLIP features are extracted, SegSplat maintains a total inference time under 0.2 seconds, making it suitable for real-time tasks.

Component	SegSplat (s)	LangSplat (s)
2D Semantic Feature Extraction	9.7000	9.7000
Semantic Gaussians Prediction	0.0284	565.0236
Gaussian Rasterization	0.0013	0.0016
Language Feature Decoder	0.0004	0.0001
Text Querying	0.0003	0.0002
Total	9.7304	575.1255

This efficiency makes SegSplat highly suitable for real-time or on-the-fly 3D scene segmentation applications, particularly in dynamic or large-scale environments.

Limitations. Despite its advancements, SegSplat has limitations defining future research directions. Its semantic understanding quality is tied to the performance of the underlying 2D foundation models (SAM and CLIP) and the K-Means clustering used for its semantic bank. A key challenge is our current reliance on aggregating per-image 2D semantic predictions without a learned 3D fusion mechanism to optimally handle view inconsistencies or occlusions during the 2D-to-3D lifting process. Additionally, geometric accuracy is inherited from the frozen DepthSplat backbone, and the system currently focuses on static scenes. Consequently, while SegSplat offers significant efficiency with sparse inputs, its semantic segmentation accuracy lags behind methods that perform per-scene optimization using more extensive view information, a trade-off inherent to its feed-forward design.

5 CONCLUSION

We have introduced SegSplat, a novel framework designed to bridge the gap between rapid, feed-forward 3D reconstruction and rich, open-vocabulary semantic understanding. By constructing a compact semantic memory bank from multi-view 2D foundation model features and predicting discrete semantic indices alongside geometric and appearance attributes for each 3D Gaussian in a single pass, SegSplat efficiently imbues scenes with queryable semantics. Our experiments demonstrate that SegSplat achieves geometric fidelity comparable to state-of-the-art feed-forward 3D Gaussian Splatting methods while simultaneously enabling robust open-set semantic segmentation, crucially *without* requiring any per-scene optimization for semantic feature integration. This work represents a significant step towards practical, on-the-fly generation of semantically aware 3D environments, vital for advancing robotic interaction, augmented reality, and other intelligent systems.

REFERENCES

Rohan Chacko, Nicolai Haeni, Eldar Khaliullin, Lin Sun, and Douglas Lee. Lifting by gaussians: A simple, fast and flexible method for 3d instance segmentation. In *Winter Conference on Applications*

of Computer Vision (WACV), 2025.

Xuweiyi Chen, Tian Xia, Sihan Xu, Jianing Yang, Joyce Chai, and Zezhou Cheng. Sab3r: Semantic-augmented backbone in 3d reconstruction. *arXiv preprint arXiv:2506.02112*, 2025.

Yuedong Chen, Haofei Xu, Chuanxia Zheng, Bohan Zhuang, Marc Pollefeys, Andreas Geiger, Tat-Jen Cham, and Jianfei Cai. MVSplat: Efficient 3d gaussian splatting from sparse multi-view images. *arXiv preprint arXiv:2403.14627*, 2024.

Zhiwen Fan, Jian Zhang, Wenyan Cong, Peihao Wang, Renjie Li, Kairun Wen, Shijie Zhou, Achuta Kadambi, Zhangyang Wang, Danfei Xu, et al. Large spatial model: End-to-end unposed images to semantic 3d. *Advances in neural information processing systems*, 37:40212–40229, 2024.

Bernhard Kerbl, Georgios Kopanas, Thomas Leimkühler, and George Drettakis. 3d gaussian splatting for real-time radiance field rendering. *ACM Trans. Graph.*, 42(4):139–1, 2023.

Justin Kerr, Chung Min Kim, Ken Goldberg, Angjoo Kanazawa, and Matthew Tancik. Lerf: Language embedded radiance fields. In *Proceedings of the IEEE/CVF International Conference on Computer Vision*, pp. 19729–19739, 2023.

Alexander Kirillov, Eric Mintun, Nikhila Ravi, Hanzi Mao, Chloe Rolland, Laura Gustafson, Tete Xiao, Spencer Whitehead, Alexander C Berg, Wan-Yen Lo, et al. Segment anything. In *Proceedings of the IEEE/CVF international conference on computer vision*, pp. 4015–4026, 2023.

Sosuke Kobayashi, Eiichi Matsumoto, and Vincent Sitzmann. Decomposing nerf for editing via feature field distillation. *Advances in neural information processing systems*, 35:23311–23330, 2022.

Boyi Li, Kilian Q Weinberger, Serge Belongie, Vladlen Koltun, and René Ranftl. Language-driven semantic segmentation. *arXiv preprint arXiv:2201.03546*, 2022.

Feng Liang, Bichen Wu, Xiaoliang Dai, Kunpeng Li, Yinan Zhao, Hang Zhang, Peizhao Zhang, Peter Vajda, and Diana Marculescu. Open-vocabulary semantic segmentation with mask-adapted clip. In *Proceedings of the IEEE/CVF Conference on Computer Vision and Pattern Recognition*, pp. 7061–7070, 2023.

Kunhao Liu, Fangneng Chen, Hengshuang Zhao, and Qi Ji. Weakly supervised 3d open-vocabulary segmentation with masked image modeling and text-image pairs. In *Advances in Neural Information Processing Systems (NeurIPS)*, 2023a.

Shilong Liu, Zhaoyang Zeng, Tianhe Ren, Feng Li, Hao Zhang, Jie Yang, Chunyuan Li, Jianwei Yang, Hang Su, Jun Zhu, et al. Grounding dino: Marrying dino with grounded pre-training for open-set object detection. *arXiv preprint arXiv:2303.05499*, 2023b.

Ben Mildenhall, Pratul P. Srinivasan, Matthew Tancik, Jonathan T. Barron, Ravi Ramamoorthi, and Ren Ng. NeRF: Representing scenes as neural radiance fields for view synthesis. In *European Conference on Computer Vision (ECCV)*, pp. 405–421. Springer, 2020.

Minghan Qin, Wanhua Li, Jiawei Zhou, Haoqian Wang, and Hanspeter Pfister. Langsplat: 3d language gaussian splatting. In *Proceedings of the IEEE/CVF Conference on Computer Vision and Pattern Recognition*, pp. 20051–20060, 2024.

Alec Radford, Jong Wook Kim, Chris Hallacy, Aditya Ramesh, Gabriel Goh, Sandhini Agarwal, Girish Sastry, Amanda Askell, Pamela Mishkin, Jack Clark, et al. Learning transferable visual models from natural language supervision. In *International conference on machine learning*, pp. 8748–8763. PMLR, 2021.

Christoph Schuhmann, Romain Beaumont, Richard Vencu, Cade W Gordon, Ross Wightman, Mehdi Cherti, Theo Coombes, Aarush Katta, Clayton Mullis, Mitchell Wortsman, Patrick Schramowski, Srivatsa R Kundurthy, Katherine Crowson, Ludwig Schmidt, Robert Kaczmarczyk, and Jenia Jitsev. LAION-5b: An open large-scale dataset for training next generation image-text models. In *Thirty-sixth Conference on Neural Information Processing Systems Datasets and Benchmarks Track*, 2022. URL <https://openreview.net/forum?id=M3Y74vmsMcY>.

Jin-Chuan Shi, Miao Wang, Hao-Bin Duan, and Shao-Hua Guan. Language embedded 3d gaussians for open-vocabulary scene understanding. *arXiv preprint arXiv:2311.18482*, 2023.

Yunyang Xiong, Bala Varadarajan, Lemeng Wu, Xiaoyu Xiang, Fanyi Xiao, Chenchen Zhu, Xiaoliang Dai, Dilin Wang, Fei Sun, Forrest Landola, et al. Efficientsam: Leveraged masked image pretraining for efficient segment anything. In *Proceedings of the IEEE/CVF Conference on Computer Vision and Pattern Recognition*, pp. 16111–16121, 2024.

Haofei Xu, Songyou Peng, Fangjinhua Wang, Hermann Blum, Daniel Barath, Andreas Geiger, and Marc Pollefeys. Depthsplat: Connecting gaussian splatting and depth. *arXiv preprint arXiv:2410.13862*, 2024.

Jiarui Xu, Sifei Liu, Arash Vahdat, Wonmin Byeon, Xiaolong Wang, and Shalini De Mello. Open-vocabulary panoptic segmentation with text-to-image diffusion models. In *Proceedings of the IEEE/CVF Conference on Computer Vision and Pattern Recognition*, pp. 2955–2966, 2023.

Botao Ye, Sifei Liu, Haofei Xu, Xuetong Li, Marc Pollefeys, Ming-Hsuan Yang, and Songyou Peng. No pose, no problem: Surprisingly simple 3d gaussian splats from sparse unposed images. *ICLR 2025*, 2024a.

Mingqiao Ye, Martin Danelljan, Fisher Yu, and Lei Ke. Gaussian grouping: Segment and edit anything in 3d scenes. In *European Conference on Computer Vision*, pp. 162–179. Springer, 2024b.

Vickie Ye, Ruilong Li, Justin Kerr, Matias Turkulainen, Brent Yi, Zhuoyang Pan, Otto Seiskari, Jianbo Ye, Jeffrey Hu, Matthew Tancik, and Angjoo Kanazawa. gsplat: An open-source library for gaussian splatting. *Journal of Machine Learning Research*, 26(34):1–17, 2025.

Chandan Yeshwanth, Yueh-Cheng Liu, Matthias Nießner, and Angela Dai. Scannet++: A high-fidelity dataset of 3d indoor scenes. In *Proceedings of the IEEE/CVF International Conference on Computer Vision*, pp. 12–22, 2023.

Alex Yu, Vickie Ye, Matthew Tancik, and Angjoo Kanazawa. pixelnerf: Neural radiance fields from one or few images. In *Proceedings of the IEEE/CVF Conference on Computer Vision and Pattern Recognition (CVPR)*, pp. 4578–4587, 2021.

Qian Zhou, Torsten Sattler, Laura Leal-Taixé, Thomas Funkhouser, and Steven M. Seitz. Realestate10k dataset. <https://google.github.io/realestate10k/>, 2018.

A APPENDIX

You may include other additional sections here.